Spectra and energy levels of ions in the zinc isoelectronic sequence from Rb VIII to Mo XIII

Ulf Litzén
Department of Physics, University of Lund, Lund, Sweden

Joseph Reader
National Bureau of Standards, Gaithersburg, Maryland 20899
(Received 12 June 1987)

Spectra of the zinclike ions Rb VIII, Sr IX, Y X, Zr XI, Nb XII, and Mo XIII were excited with sparks and laser-produced plasmas and observed with normal- and grazing-incidence vacuum spectrographs. Almost all levels of the $4s^2$, $4s4p$, $4p^2$, $4s4d$, $4s5s$, $4s5p$, $4p5s$, and $4s5d$ configurations were established in these ions. Several $4s4f\ ^3F-4s5g\ ^3G$ transitions of Nb XII and Mo XIII were also identified. The observed energy levels were interpreted by means of least-squares parametric fits and Hartree-Fock calculations. The ionization energies were determined as 132.79(25) eV for Rb VIII, 158.33(25) eV for Sr IX, 185.77(37) eV for Y X, 214.86(37) eV for Zr XI, 246.11(37) eV for Nb XII, and 279.09(50) eV for Mo XIII.

Ions of the Zn isoelectronic sequence have the ground configuration $3d^{10}4s^2$. Recently, Litzén and Ando[1] excited spectra of Zr XI, Nb XII, and Mo XIII with a laser-produced plasma and established the complete $4s4p$ and $4p^2$ configurations of these ions. This provided the first excited levels for these ions, other than levels connected to the $4s^2\ ^1S_0$ ground state by resonance transitions. In earlier work, Alexander *et al.*[2] reported the $4s^2\ ^1S_0-4s5p\ ^{1,3}P_1$ resonance lines of Y X, Zr XI, Nb XII, Mo XIII and three $4s4p\ ^3P-4s5s\ ^3S$ transitions of Mo XIII. The $4s^2\ ^1S_0-4s4p\ ^1P_1$ resonance transition of Mo XIII was first observed by Hinnov *et al.*[3] with a tokamak light source. It is now being used routinely for tokamak diagnostics.[4] The identification of this line was confirmed by Reader and Acquista,[5] who observed it in the six ions from Rb VIII to Mo XIII. The $4s^2\ ^1S_0-4s4p\ ^3P_1$ and $4s^2\ ^1S_0-4s4p\ ^3P_2$ resonance lines and three transitions of the type $4s4p$-$4p^2$ of Mo XIII were observed in a tokamak by Finkelthal *et al.*[6] However, only the $4s^2\ ^1S_0-4s4p\ ^3P_1$ and $4s4p\ ^3P_2-4p^2\ ^3P_2$ identifications were found to be correct by Litzén and Ando.[1] Inner-shell excitations of the type $3d^{10}4s^2$-$3d^9 4s^2 4p$ have been observed in Mo XIII by Burkhalter *et al.*,[7] in Y X–Mo XIII by Wyart *et al.*,[8] in Sr IX by Acquista and Reader,[9] and in Rb VIII by Wyart *et al.*[10]

In the present work, we observed spectra of Zn-like ions from Rb VIII to Mo XIII with sparks and laser-produced plasmas and extended the analyses to include most of the levels of the $4s^2$, $4s4p$, $4p^2$, $4s4d$, $4s5s$, $4s5p$, $4s5d$, and $4p5s$ configurations. Several $4s4f$-$4s5g$ transitions of Nb XII and Mo XIII were also identified. Revised values were obtained for the $4s4p\ ^3P_0$ levels of Zr XI, Nb XII, and Mo XIII, based originally[1] on the identification of single transitions. The previous identifications[2] of the $4s4p$-$4s5s$ transitions of Mo XIII were also revised.

EXPERIMENT

Most of the present measurements were taken from earlier observations at the National Bureau of Standards (NBS). The spectra were excited in a low-inductance vacuum spark at voltages ranging from 1 to 15 kV and photographed with the NBS 10.7-m grazing-incidence spectrograph. The grating had 1200 lines/mm; the plate factor at 300 Å was 0.25 Å/mm. The ionization stages of the lines were distinguished by comparing their shapes and relative intensities at different discharge voltages. More complete experimental details, including reference spectra, are given in previous reports on Cu-like ions.[9,11–16]

In order to observe intercombination lines lying at relatively long wavelengths, new observations of the present ions were made with normal-incidence spectrographs. For Rb VIII, spectra of RbCl, RbI, and Rb_2CO_3 were excited in a low-voltage sliding spark and photographed with the NBS 10.7-m normal-incidence spectrograph. The grating contained 1200 lines/mm; the plate factor was 0.78 Å/mm. Lines of Rb VIII were excited at a peak current in the spark of about 2500 Å. The wavelength measurements were taken from the spectrum of Rb_2CO_3. Reference spectra consisted of lines of C II,[17,18] O II,[18] O III,[19] Al III,[20] Rb II,[21] Rb III,[22] Rb IV,[23] and Rb V.[24] For ions from Sr IX to Mo XIII, spectra were recorded with the 3-m normal-incidence spectrograph at the University of Lund. The grating contained 1200 lines/mm and the plate factor was 2.75 Å/mm. The spectra were produced by focussing the light from a Nd:YAG/glass laser onto flat targets (where YAG denotes yttrium aluminum garnet). Laser pulses had an energy of 4 J and a duration of 3 nsec. Ten shots were used for each spectrum. Reference spectra consisted of lines of the Cu-like ions[9,11–16] appearing in second or-

TABLE I. Observed lines of Zn-like ions from Rb VIII to Mo XIII.

Transition	Rb VIII		Sr IX		Y X		Zr XI		Nb XII		Mo XIII	
	λ (Å)	Intensity[a]	λ (Å)	Intensity	λ (Å)	Intensity	λ (Å)	Intensity	λ (Å)	Intensity	λ (Å)	Intensity
$4s^2\,{}^1S_0-4s5p\,(1/2,3/2)_1$	169.361	100	145.014	100	126.049	100	110.746	100	98.204	100	87.770	100
$4s^2\,{}^1S_0-4s5p(1/2,1/2)_1$	170.625	50	146.364	50	127.255	50	111.863	50	99.250	50	88.756	50
$4s4p\,{}^3P_0-4s5d\,{}^3D_1$					132.700	20	115.986	10	102.418	12	91.187	10
$4s4p\,{}^3P_1-4s5d\,{}^3D_2$			154.553	5	133.450	45	116.654	20	103.016	20	91.752	40
$4s4p\,{}^3P_1-4s5d\,{}^3D_1$					133.570	15	116.768	10	103.127	10	91.834	15
$4s4p\,{}^3P_2-4s5d\,{}^3D_3$			156.932	25	135.603	45	118.640	50	104.872	70	93.493	75
$4s4p\,{}^3P_2-4s5d\,{}^3D_2$					135.793	20	118.840	10	105.071	10	93.696	6
$4s4p\,{}^3P_0-4s5s\,{}^3S_1$	255.573	100	214.253	100	182.624	70	157.783	75	137.859	100	121.597	150
$4s4p\,{}^3P_1-4s5s\,{}^3S_1$	257.791	200	216.151	300*p*	184.271	200	159.231	150	139.145	250	122.746	300
$4s4p\,{}^3P_2-4s5s\,{}^3S_1$	263.412	400	221.123	500	188.745	350	163.307	300	142.915	500	126.258	500
$4s4p\,{}^1P_1-4s5s\,{}^1S_0$	290.915	75	241.566	125	204.441	150	175.682	100	152.872	100	134.428	500
$4p^2\,{}^1D_2-4p5s\,(3/2,1/2)_1$			216.125	20	184.192	35	159.114	50*p*	138.997	30	122.577	30
$4p^2\,{}^3P_1-4p5s\,(3/2,1/2)_2$			217.809	5	185.460	45	160.077	75	139.740	20	123.182	30
$4p^2\,{}^1D_2-4p5s\,(3/2,1/2)_2$			218.349	25	185.973	45	160.550	50*p*	140.183	40	123.558	30
$4p^2\,{}^3P_0-4p5s\,(1/2,1/2)_1$					187.586	35	161.894	30	141.325	35	124.541	30*p*
$4p^2\,{}^3P_2-4p5s\,(3/2,1/2)_1$			222.481	30	189.871	50	164.245	75	143.704	40	126.930	150
$4p^2\,{}^3P_1-4p5s\,(1/2,1/2)_1$			224.173	50	191.165	30	165.252	20	144.502	20	127.575	35
$4p^2\,{}^1D_2-4p5s\,(1/2,1/2)_1$			224.745	45	191.707	70	165.753	60	144.959[b]	200*w*	127.983[b]	300
$4p^2\,{}^3P_2-4p5s\,(3/2,1/2)_2$			224.843	45	191.764	75	165.785	65	144.959[b]	200*w*	127.983[b]	300
$4p^2\,{}^3P_1-4p5s\,(1/2,1/2)_0$			224.909	30	191.885	70	165.863	30	145.025	30	128.028	50
$4p^2\,{}^1S_0-4p5s\,(3/2,1/2)_1$					205.741	15	176.543	20	153.431	30	134.763	15
$4s4f\,{}^3F_2-4s5g\,{}^3G_3$									240.406	40	204.017	50
$4s4f\,{}^3F_3-4s5g\,{}^3G_4$									240.460	50	204.059	70
$4s4f\,{}^3F_4-4s5g\,{}^3G_5$									240.523	60	204.137	100
$4s4p\,{}^3P_1-4s4d\,{}^1D_2$			303.966	150	274.976	50	250.979	35	230.754	200	213.397	200
$4s4p\,{}^3P_0-4s4d\,{}^3D_1$	377.818	1000	336.974	750	304.054	300	276.860	500	253.971	50	234.415	200
$4s4p\,{}^3P_1-4s4d\,{}^3D_2$	381.787	3000	340.776	700	307.699	1000*bl*	280.382	700*w*	257.349	50	237.685	250
$4s4p\,{}^3P_1-4s4d\,{}^3D_1$	382.678	500	341.687	500	308.650	300	281.359	200	258.380	100	238.737	100
$4s4p\,{}^3P_2-4s4d\,{}^3D_3$	392.786	5000	351.754	900	318.752	800	291.565	500	268.758	150	249.306	100
$4s4p\,{}^3P_2-4s4d\,{}^3D_2$	394.257	500	353.305	300	320.385	75	293.293	300	270.560	40*p*		
$4s4p\,{}^1P_1-4s4d\,{}^1D_2$	419.667	1000	373.648	500	336.991	500	307.048	300	282.078	120	260.923	300
$4s4p\,{}^3P_1-4p^2\,{}^3P_2$	528.390	500	473.883	300	428.284	300	389.476	100	355.981	300	326.741	100
$4s4p\,{}^3P_2-4p^2\,{}^3P_2$	552.562	600	498.458	400	453.263	200	414.855	500	381.733	800	352.868	800
$4s4p\,{}^3P_0-4p^2\,{}^3P_1$	551.807	400	498.135	250	453.193	150	414.911	300	381.855	200	352.994	200

TABLE I. (*Continued*).

Transition	Rb VIII λ (Å)	Rb VIII Intensity[a]	Sr IX λ (Å)	Sr IX Intensity	Y X λ (Å)	Y X Intensity	Zr XI λ (Å)	Zr XI Intensity	Nb XII λ (Å)	Nb XII Intensity	Mo XIII λ (Å)	Mo XIII Intensity
$4s4p\ ^3P_1-4p^2\ ^1D_2$	559.947	100	505.625	100	460.313	50	421.806	200	388.595	200	359.643	200
$4s4p\ ^3P_1-4p^2\ ^3P_1$	562.253	200	508.513	100	463.480	50	425.087	100	391.898	400	362.889	150
$4s4p\ ^1P_1-4p^2\ ^1S_0$	587.669	150	530.566	150	482.622	25	441.675	70	406.235	200	375.243	75
$4s4p\ ^3P_1-4p^2\ ^3P_0$	581.809	200	529.491	300	485.933	30	449.048	150	417.401	200	389.929	500
$4s4p\ ^3P_2-4p^2\ ^1D_2$	587.165	250	533.701	400	489.291	75	451.738	300	419.524	200*p*	391.552	750
$4s4p\ ^3P_2-4p^2\ ^3P_1$	589.699	250	536.915	300	492.870	50	455.494	200	423.352	200	395.400	500
$4s4p\ ^1P_1-4p^2\ ^3P_2$	750.333	50	668.11	100	600.355	30	543.41	150	494.92	150	453.09	150
$4s4p\ ^1P_1-4p^2\ ^1D_2$	815.584	200	733.01	75	665.30	20	608.44	100	560.31	100	518.92	200
$4s^2\ ^1S_0-4s4p\ ^1P_1$	524.929	10 000	475.336	2500	433.785	2000	398.357	5000	367.730	4000	340.909	4000
$4s^2\ ^1S_0-4s4p\ ^3P_1$	743.369	500	671.06	50	611.217	10	560.84	75	517.93	50	480.85	100

[a]Symbols: *p*, perturbed; *w*, wide; *bl*, blend.
[b]Doubly classified.

der.

The wavelengths, intensities, and classifications of the observed lines are given in Table I. The intensities are visual estimates of plate blackening. The wavelengths of lines measured with the 10.7-m spectrographs at NBS have an estimated uncertainty of ±0.005 Å. They are given to three decimal places in the table. Because of the difficulty of finding a sufficient number of unblended reference lines in the long-wavelength region, the lines observed with the 3-m spectrograph in Lund could not be as well measured. The estimated wavelength uncertainty of these lines is ±0.02 Å. They are given to two decimal places in Table I. Our wavelength for the $4s^2\ ^1S_0-4s4p\ ^1P_1$ transition of Sr IX, 475.336 Å, represents a revision of Reader and Acquista's[5] value of 475.358 Å. A similar revision was found for the 4*s*-4*p* transitions of the Cu-like ion Sr X,[9] where the discrepancy was ascribed to possible spectrograph illumination effects for $n=4$-4 transitions.

LINE IDENTIFICATIONS AND ENERGY LEVELS

The line identifications were carried out with the aid of isoelectronic comparisons and *ab initio* calculations of the level structures and transition wavelengths. In most cases the identifications were confirmed by recurring wave-number intervals.

The energy levels are given in Tables II–VII. The level values were determined by a least-squares optimization procedure with the computer code ELCALC.[25] Blended or otherwise perturbed lines were given a low weight or excluded from the optimization. This was also true of lines in the long-wavelength region mentioned above. The uncertainties of the level values as calculated by the optimization code are given in the tables.

An overview of the configurations and transitions involved in the present work is shown for Mo XIII in Fig. 1. It can be seen that certain transitions that we might have expected to observe were in fact not found. For example, the $J=1$ levels of the $4s5p$ configuration are known through their strong transitions to the ground state, and the wavelengths of their transitions to known levels of $4s4d$ can be calculated exactly. However, these transitions were not observed. Other possible transitions from $4s5p$ to $4s4d$ were similarly not observed.

Transitions of the type $4p^2$-$4p4d$ and $4s4d$-$4s4f$ were also not identified. These lines appear together with a tremendous number of $n=4$-4 transitions of several ionization states, and we have not as yet been able to make any positive identifications for them. The $4s4f$-$5s5g$ transitions of Rb VIII–Zr XI are expected to appear in this same complex region, and they have also not been identified. In Nb XII and Mo XIII, the $4f$-$5g$ transitions are displaced to shorter wavelength, and for these ions the $4f\ ^3F-5g\ ^3G$ transitions could be located. These identifications were aided by comparison of the spark spectra with laser-produced spectra from NBS that contained only a limited number of ionization stages.

Our identification of $4s4p\ ^3P_0-4p^2\ ^3P_1$ in Zr XI, Nb XII, and Mo XIII differs from that given in Ref. 1. In Ref. 1 this line was blended with the strong $4s4p\ ^3P_2-4p^2\ ^3P_2$ transition and could not be detected.

TABLE II. Energy levels of Rb VIII (in cm^{-1}).

Term	J	E	Uncertainty	Interval
$4s^2\,{}^1S$	0	0	1	
$4s4p\,{}^3P$	0	131 157	2	3366
$4s4p\,{}^3P$	1	134 523	1	8279
$4s4p\,{}^3P$	2	142 802	1	
$4s4p\,{}^1P$	1	190 501	1	
$4p^2\,{}^3P$	0	306 401	2	5978
$4p^2\,{}^3P$	1	312 379	1	11 397
$4p^2\,{}^3P$	2	323 776	1	
$4p^2\,{}^1D$	2	313 112	1	
$4p^2\,{}^1S$	0	360 665	2	
$4s4d\,{}^3D$	1	395 837	3	609
$4s4d\,{}^3D$	2	396 446	3	948
$4s4d\,{}^3D$	3	397 394	3	
$4s4d\,{}^1D$	2	428 785	3	
$4s5s\,{}^3S$	1	522 435	4	
$4s5s\,{}^1S$	0	534 244	6	
$4s5p(1/2,1/2)$	1	586 081	17	
$4s5p(1/2,3/2)$	1	590 455	17	

TABLE III. Energy levels of Sr IX (in cm^{-1}).

Term	J	E	Uncertainty	Interval
$4s^2\,{}^1S$	0	0	3	
$4s4p\,{}^3P$	0	144 933	2	4096
$4s4p\,{}^3P$	1	149 029	1	10404
$4s4p\,{}^3P$	2	159 433	1	
$4s4p\,{}^1P$	1	210 378	2	
$4p^2\,{}^3P$	0	337 890	2	7792
$4p^2\,{}^3P$	1	345 682	1	14 370
$4p^2\,{}^3P$	2	360 052	2	
$4p^2\,{}^1D$	2	346 804	2	
$4p^2\,{}^1S$	0	398 856	3	
$4s4d\,{}^3D$	1	441 693	3	783
$4s4d\,{}^3D$	2	442 476	3	1247
$4s4d\,{}^3D$	3	443 723	4	
$4s4d\,{}^1D$	2	478 011	4	
$4s5s\,{}^3S$	1	611 668	7	
$4s5s\,{}^1S$	0	624 344	9	
$4s5p(1/2,1/2)$	1	683 228	24	
$4s5p(1/2,3/2)$	1	689 589	24	
$4s5d\,{}^3D$	1			
$4s5d\,{}^3D$	2	796 056	21	596
$4s5d\,{}^3D$	3	796 652	20	
$4p5s(1/2,1/2)$	0	790 306	10	1468
$4p5s(1/2,1/2)$	1	791 774	9	
$4p5s(3/2,1/2)$	2	804 797	10	4718
$4p5s(3/2,1/2)$	1	809 515	13	

TABLE IV. Energy levels of Y X (in cm^{-1}).

Term	J	E	Uncertainty	Interval
$4s^2\,{}^1S$	0	0	2	
$4s4p\,{}^3P$	0	158 709	3	4898
$4s4p\,{}^3P$	1	163 607	1	12 867
$4s4p\,{}^3P$	2	176 474	2	
$4s4p\,{}^1P$	1	230 530	2	
$4p^2\,{}^3P$	0	369 397	3	9969
$4p^2\,{}^3P$	1	379 366	2	17 731
$4p^2\,{}^3P$	2	397 097	2	
$4p^2\,{}^1D$	2	380 850	2	
$4p^2\,{}^1S$	0	437 731	3	
$4s4d\,{}^3D$	1	487 598	4	1000
$4s4d\,{}^3D$	2	488 598	5	1601
$4s4d\,{}^3D$	3	490 199	5	
$4s4d\,{}^1D$	2	527 274	4	
$4s5s\,{}^3S$	1	706 286	9	
$4s5s\,{}^1S$	0	719 669	12	
$4s5p(1/2,1/2)$	1	785 824	31	
$4s5p(1/2,3/2)$	1	793 342	32	
$4s5d\,{}^3D$	1	912 284	20	635
$4s5d\,{}^3D$	2	912 919	29	1002
$4s5d\,{}^3D$	3	913 921	27	
$4p5s(1/2,1/2)$	0	900 511	14	1969
$4p5s(1/2,1/2)$	1	902 480	9	
$4p5s(3/2,1/2)$	2	918 566	9	5205
$4p5s(3/2,1/2)$	1	923 771	9	

The evolution of the observed $4s4l$ configurations along the isoelectronic sequence is shown in Fig. 2.

THEORETICAL CALCULATIONS

Ab initio calculations of the energy-level structures were made with the Cowan code[26] using HXR (Hartree exchange with relativity) wave functions. The calculations included all configurations of the $n=4$ complex, that is, the even configurations $4s^2$, $4s4d$, $4p^2$, $4p4f$, $4d^2$, $4f^2$ and the odd configurations $4s4p$, $4s4f$, $4p4f$, $4p4d$, $4d4f$. Calculations were also carried out for the $4s5s$, $4s5p$, $4s5d$, $4s5f$, and $4s5g$ configurations. Separate calculations for Y X included the $4p5s$, $4p5p$, and $4p5d$ configurations. The calculated structures show good agreement with the observations. In each ion the average energies of the configurations differ from the observations by approximately the same amount, so the predicted wavelengths deviate from the observations by only a few angstroms.

Predicted values for the levels of the $4s^2$, $4s4p$, $4p^2$, $4s4d$, and $4p4d$ configurations of ions in the Zn sequence from $Z=37-50$ have recently been reported by Ivanova *et al.*[27] Their predictions agree fairly well with our observed values.

TABLE V. Energy levels of Zr XI (in cm^{-1}).

Term	J	E	Uncertainty	Interval
$4s^2\,{}^1S$	0	0	4	
$4s4p\,{}^3P$	0	172 535	3	5770
$4s4p\,{}^3P$	1	178 305	2	15 704
$4s4p\,{}^3P$	2	194 009	2	
$4s4p\,{}^1P$	1	251 031	3	
$4p^2\,{}^3P$	0	400 998	3	12 553
$4p^2\,{}^3P$	1	413 551	2	21 507
$4p^2\,{}^3P$	2	435 058	3	
$4p^2\,{}^1D$	2	415 381	3	
$4p^2\,{}^1S$	0	477 442	4	
$4s4d\,{}^3D$	1	533 725	5	1238
$4s4d\,{}^3D$	2	534 963	5	2023
$4s4d\,{}^3D$	3	536 986	6	
$4s4d\,{}^1D$	2	576 713	6	
$4s5s\,{}^3S$	1	806 332	15	
$4s5s\,{}^1S$	0	820 241	16	
$4s5p(1/2,1/2)$	1	893 951	40	
$4s5p(1/2,3/2)$	1	902 967	41	
$4s5d\,{}^3D$	1	1 034 706	26	802
$4s5d\,{}^3D$	2	1 035 508	34	1387
$4s5d\,{}^3D$	3	1 036 895	36	
$4p5s(1/2,1/2)$	0	1 016 458	18	2229
$4p5s(1/2,1/2)$	1	1 018 687	11	
$4p5s(3/2,1/2)$	2	1 038 249	13	5639
$4p5s(3/2,1/2)$	1	1 043 888	16	

TABLE VI. Energy levels of Nb XII (in cm^{-1}).

Term	J	E	Uncertainty	Interval
$4s^2\,{}^1S$	0	0	4	
$4s4p\,{}^3P$	0	186 363	4	6714
$4s4p\,{}^3P$	1	193 077	2	18 956
$4s4p\,{}^3P$	2	212 033	3	
$4s4p\,{}^1P$	1	271 939	3	
$4p^2\,{}^3P$	0	432 655	4	15 589
$4p^2\,{}^3P$	1	448 244	3	25 749
$4p^2\,{}^3P$	2	473 993	3	
$4p^2\,{}^1D$	2	450 413	3	
$4p^2\,{}^1S$	0	518 102	4	
$4s4d\,{}^3D$	1	580 106	6	1544
$4s4d\,{}^3D$	2	581 650	8	2465
$4s4d\,{}^3D$	3	584 115	8	
$4s4d\,{}^1D$	2	626 447	7	
$4s5s\,{}^3S$	1	911 748	15	
$4s5s\,{}^1S$	0	926 081	22	
$4s5p(1/2,1/2)$	1	1 007 557	51	
$4s5p(1/2,3/2)$	1	1 018 288	52	
$4s5d\,{}^3D$	1	1 162 754	34	1030
$4s5d\,{}^3D$	2	1 163 784	34	1792
$4s5d\,{}^3D$	3	1 165 576	46	
$4p5s(1/2,1/2)$	0	1 137 780	24	2481
$4p5s(1/2,1/2)$	1	1 140 261	21	
$4p5s(3/2,1/2)$	2	1 163 812	37	6049
$4p5s(3/2,1/2)$	1	1 169 861	14	

The structures of the present observed configurations were analyzed through least-squares fits of the energy parameters to the observed levels. The fitted parameters were compared with energy integrals calculated with the Hartree-Fock (HF) code of Froese-Fischer[28] in the single-configuration mode. The results are discussed below.

$4s^2+4p^2+4s4d$ configurations

These configurations are known completely for all six of the present ions. The structures of the $4p^2$ and $4s4d$ configurations of Mo XIII are shown in Fig. 3. The results of fitting the complete $4s^2+4p^2+4s4d$ group of levels are given in Tables VIII and IX. It can be seen that the parameters are well defined and vary smoothly along the sequence.

The levels designated as $4p^2\,{}^1D_2$ and $4p^2\,{}^3P_2$ are highly mixed states. As seen from the tables, the lower level is designated $4p^2\,{}^1D_2$ and the higher $4p^2\,{}^3P_2$. This is in agreement with the designations of Litzén and Ando,[1] but differs from the order suggested by Ivanova *et al.*[27] The large state admixtures are reflected in the observed intensities. For example, the transitions from $4p^2\,{}^1D_2$ and $4p^2\,{}^3P_2$ to $4s4p\,{}^1P_1$ have nearly equal intensities, although the $4s4p\,{}^1P_1$ level is an almost pure singlet state. These mixed levels provide the main basis for connecting the singlet and triplet level systems.

The depression of $4p^2\,{}^1D_2$ to a point below $4p^2\,{}^3P_2$ is caused by interaction with $4s4d\,{}^1D_2$. The $4p^2\,{}^1D-4s4d\,{}^1D$ interaction found here is smaller than in the beginning of the sequence, where in Ga II (Refs. 29 and 30) the admixture is about 50%. The interaction gradually decreases with increasing Z.

The interaction between the $4s^2\,{}^1S_0$ ground state and the $4p^2\,{}^1S_0$ state cannot be determined from the observed levels, and the configuration interaction parameter $R^1(4s^2,4p^2)$ was consequently fixed at its HF value. Although the level admixtures are only abut 2%, the depression of the ground state is about 10 000 cm^{-1}. In calculating the ionization energies, it was important to take this shift in account. This was done by using the fitted value of $E_{av}(4s^2)$ as the position of the configuration in the series calculation.

In the plot of $4p^2\,{}^1S_0$ in Fig. 2 points were omitted for As IV (Ref. 31) and Br VI.[32] These points deviate from the curve significantly and are evidently not correct.

TABLE VII. Energy levels of Mo XIII (in cm^{-1}).

Term	J	E	Uncertainty	Interval
$4s^2\,{}^1S$	0	0	6	
$4s4p\,{}^3P$	0	200 259	4	7723
$4s4p\,{}^3P$	1	207 982	2	22 660
$4s4p\,{}^3P$	2	230 642	3	
$4s4p\,{}^1P$	1	293 333	4	
$4p^2\,{}^3P$	0	464 439	4	19 110
$4p^2\,{}^3P$	1	483 549	3	30 485
$4p^2\,{}^3P$	2	514 034	3	
$4p^2\,{}^1D$	2	486 036	3	
$4p^2\,{}^1S$	0	559 827	5	
$4s4d\,{}^3D$	1	626 853	7	1854
$4s4d\,{}^3D$	2	628 707	9	3048
$4s4d\,{}^3D$	3	631 755	8	
$4s4d\,{}^1D$	2	676 590	7	
$4s5s\,{}^3S$	1	1 022 664	20	
$4s5s\,{}^1S$	0	1 037 226	28	
$4s5p(1/2,1/2)$	1	1 126 684	64	
$4s5p(1/2,3/2)$	1	1 139 342	65	
$4s5d\,{}^3D$	1	1 296 905	42	996
$4s5d\,{}^3D$	2	1 297 901	44	2339
$4s5d\,{}^3D$	3	1 300 240	57	
$4p5s(1/2,1/2)$	0	1 264 629	31	2773
$4p5s(1/2,1/2)$	1	1 267 402	31	
$4p5s(3/2,1/2)$	2	1 295 364	24	6500
$4p5s(3/2,1/2)$	1	1 301 864	18	

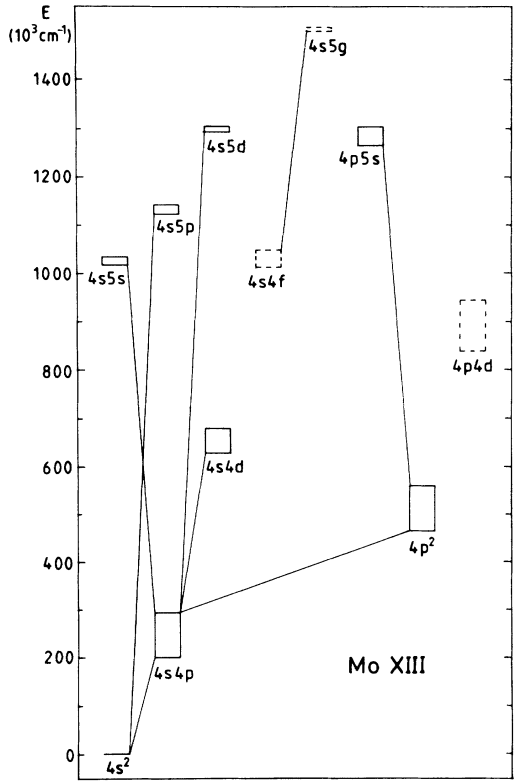

FIG. 1. Configurations and transitions of Mo XIII involved in the present work. Predicted positions are shown for $4p4d$, which was not found, and for $4s4f$ and $4s5g$, which were not connected to the rest of the level system.

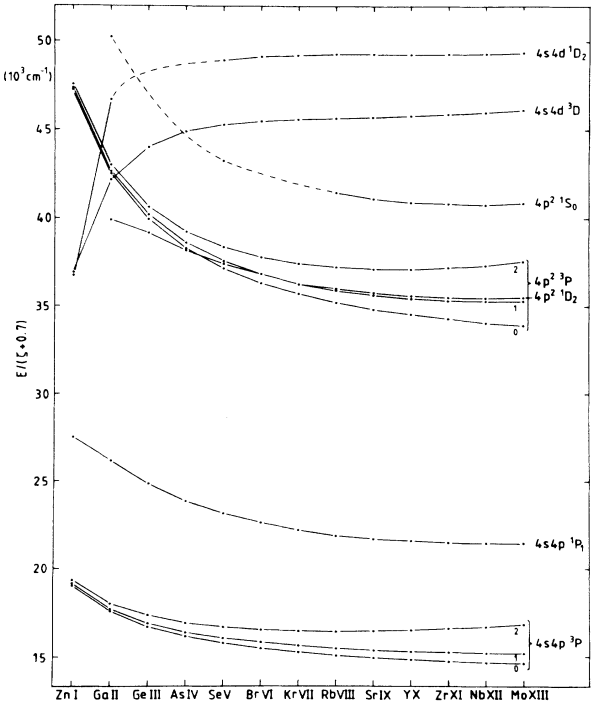

FIG. 2. Evolution of $4l4l'$ configurations in Zn isoelectronic sequence. ζ is the net charge of the atomic core, $\zeta = Z - N_e + 1$, where N_e is the total number of electrons.

$4s\,5s$ configuration

This configuration is also complete in all of the present ions. The fitted and HF parameters are given in Table X. With two levels and two parameters, the fit is exact.

$4s\,5d$ configuration

Although three of the $4s5d\,{}^3D$ levels were found in Y X–Mo XIII, only two $4s5d\,{}^3D$ levels were found in Sr IX, and none at all in Rb VIII. As $4s5d\,{}^1D_2$ was not found in any of the present ions, $G^2(4s5d)$ was fixed at 80% of its HF value in the least-squares fits. The resultant parameter values are given in Table XI. As can be seen, the fitted value of the spin-orbit parameter ζ_{5d} is larger than expected and varies in an irregular way. However, $4s5d$ interacts strongly with $4p5p$ and the changing mixing as $4p5p$ moves down relative to $4s5d$ may cause the irregularities.

$4s\,4p$ configuration

This configuration is complete in all of the present ions. The structure of $4s4p$ in Mo XIII is shown in Fig.

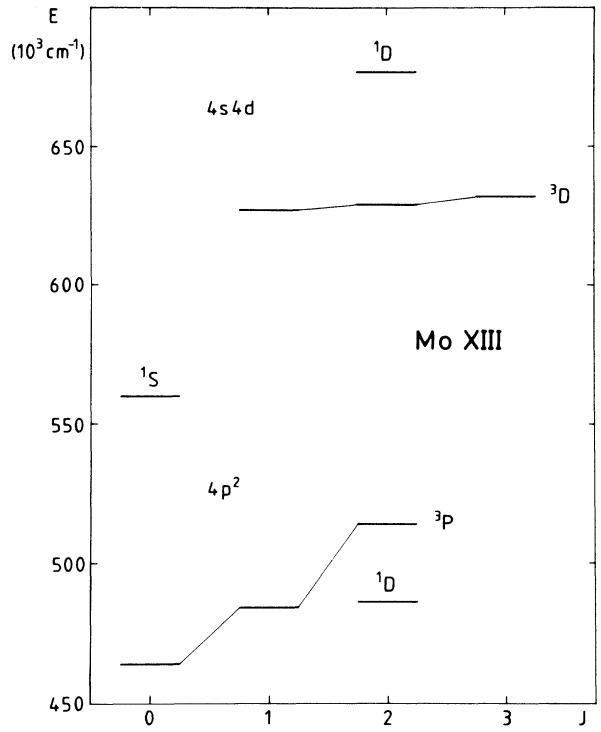

FIG. 3. Level structure of the $4p^2$ and $4s4d$ configurations of Mo XIII.

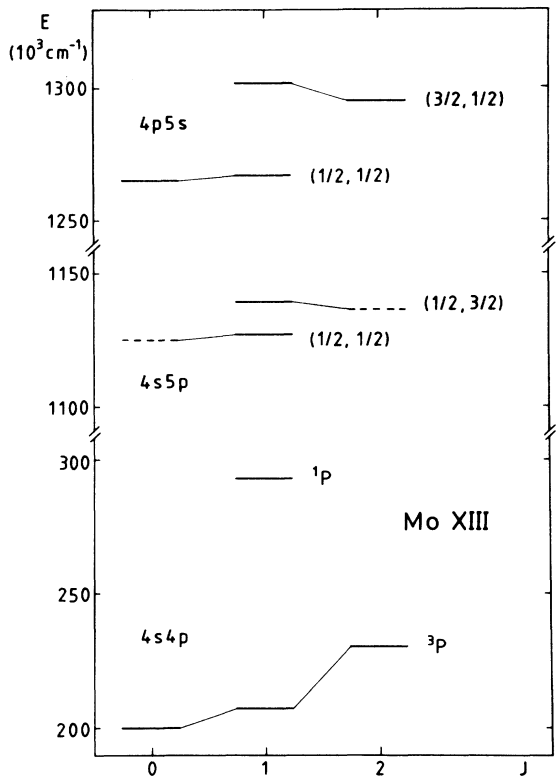

FIG. 4. Level structure of the $4s4p$, $4s5p$, and $4p5s$ configurations of Mo XIII. Predicted positions are given for the $4s5p\ ^3P_0$ and $^3P_2$ levels, which have not been established experimentally.

4. The fitted and HF parameters are given in Table XII. The fitted parameters vary smoothly through the sequence. The coupling within $4s4p$ is nearly pure LS; for the two $J=1$ levels, the ^1P-^3P mixing varies from 1% in Rb VIII to 3% in Mo XIII. Indeed, no intercombination lines are observed in the transitions to $4s5s$. Curtis[33] has recently predicted the $4s4p\ ^3P_2-{}^3P_0$ energy interval for all ions of the Zn sequence up to $Z=92$ by a semiempirical calculation. His predicted intervals agree with our observed values to within about 200 cm^{-1}.

$4s5p+4p5s$ configurations

As mentioned, only the $J=1$ levels of $4s5p$ are known. The complete $4p5s$ configuration was found in Sr IX–Mo XIII. No levels of $4p5s$ were found in Rb VIII. The structure of these two configurations in Mo XIII is shown in Fig. 4. The coupling is close to J_1j. The effect of greater spin-orbit interaction for the $4p$ electron compared to $5p$ is evident in the relative splitting between the pairs of the two configurations. Because of the missing levels of $4s5p$, some parameters had to be fixed in the least-squares calculations. As shown in Table XIII, ζ_{5p} was fixed at its HF value and the configuration-interaction integrals were fixed at 80% of their HF values. The fitted value of $G^1(4p5s)$ is unexpectedly small, and the fit for Sr IX is poor. A possible explanation for this might be interaction between $4p5s$ and $4s6p$, as is indicated by our *ab initio* calculations. Although treated together, the $4s5p$-$4p5s$ configuration mixing was found to be only about 2%.

IONIZATION ENERGIES

Ionization energies for the present ions were determined from the various two-member series shown in Table XIV. The series limits were calculated by using values for Δn^*, the change in effective quantum number between the two series members, as calculated with the Hartree-Fock computer program of Cowan,[26] including relativity and correlation corrections. The calculated values were scaled according to the observed scale factors of Δn^* found for Cu-like ions of the same ionization stage. The positions of the series members were taken to be the fitted values of the configuration average energies given in Tables VIII–XIII. The values of Δn^* and the ionization energies calculated with the different series are given in Table XIV. The uncertainty listed for each calculated ionization energy corresponds to an assumed uncertainty of ± 0.0010 in Δn^*, with no account taken of the uncertainty in the observed positions of the series members.

The adopted ionization energies are listed in Table XIV. The uncertainties of the adopted ionization energies are based on the agreement of the values found from

TABLE VIII. Fitted and Hartree-Fock parameters (in cm^{-1}) for $4s^2+4p^2+4s4d$. The first row for each parameter gives the fitted value, the second row gives the HF value, and the third row the ratio between fitted and HF values. HF values were calculated with the Froese code, Ref. 28. σ is the rms difference between the calculated and observed level values.

	Rb VIII	Sr IX	Y X	Zr XI	Nb XII	Mo XIII
$E_{av}(4s^2)$	9606±9	9915±10	10 201±11	10 469±13	10 719±13	10 955±14
	0	0	0	0	0	0
$E_{av}(4p^2)$	322 745±6	357 544±7	392 855±8	428 802±9	465 421±9	502 824±10
	290 609	320 247	349 719	379 061	408 299	437 455
	1.111	1.116	1.123	1.131	1.140	1.149
$F^2(4p4p)$	54 463±23	59 069±27	63 611±31	68 074±35	72 547±37	76 966±41
	75 674	80 996	86 186	91 271	96 271	101 200
	0.720	0.729	0.738	0.746	0.754	0.761
ζ_{4p}	7643±6	9530±6	11 691±7	14 147±8	16 928±8	20 054±8
	6714	8415	10 362	12 576	15 076	17 883
	1.139	1.133	1.128	1.125	1.123	1.121
$E_{av}(4s4d)$	401 665±6	448 429±7	495 275±8	542 363±9	589 755±9	637 564±10
	374 098	416 863	459 142	501 005	542 536	583 732
	1.074	1.076	1.079	1.083	1.087	1.092
$G^2(4s4d)$	48 934±49	55 196±58	61 173±64	66 852±72	72 383±74	77 704±81
	61 867	68 843	75 419	81 652	87 592	93 279
	0.791	0.802	0.811	0.819	0.826	0.833
ζ_{4d}	623±5	812±6	1041±6	1305±7	1602±7	1961±8
	564	754	979	1244	1552	1905
	1.105	1.077	1.063	1.049	1.032	1.029
$R^1(4s^2,4p^2)$	100 217[a]	107 063[a]	113 732[a]	120 259[a]	126 668[a]	132 979[a]
$R^1(4p^2,4s4d)$	67 989±45	74 211±55	80 268±64	86 156±73	91 959±77	97 740±86
	90 129	97 851	105 224	112 314	119 170	125 832
	0.755	0.758	0.763	0.767	0.772	0.777
σ	9	10	11	12	13	14

[a]Fixed at HF value.

TABLE IX. Percentage composition of levels of $4s^2+4p^2+4s4d$.

Level	Percentage composition in Rb VIII, Sr IX, Y X, Zr XI, Nb XII, and Mo XIII
$4s^2\,{}^1S_0$	97,98,98,98,98,98% $4s^2\,{}^1S$; 3,2,2,2,2,2% $4p^2\,{}^1S$
$4p^2\,{}^3P_0$	96,95,94,93,92,90% $4p^2\,{}^3P$; 4,5,6,7,8,9% $4p^2\,{}^1S$;
$4p^2\,{}^1S_0$	93,93,92,91,90,89% $4p^2\,{}^1S$; 4,5,6,7,8,9% $4p^2\,{}^3P$; 3,2,2,2,2,2% $4s^2\,{}^1S$
$4p^2\,{}^3P_1$	100,100,100,100,100,100% $4p^2\,{}^3P$
$4s4d\,{}^3D_1$	100,100,100,100,100,100% $4s4d\,{}^3D$
$4p^2\,{}^1D_2$	58,57,57,57,57,57% $4p^2\,{}^1D$; 35,37,37,38,38,38% $4p^2\,{}^3P$; 7,6,5,5,5,5% $4s4d\,{}^1D$
$4p^2\,{}^3P_2$	64,63,63,62,62,62% $4p^2\,{}^3P$; 31,33,33,34,34,34% $4p^2\,{}^1D$; 5,4,4,4,4,4% $4s4d\,{}^1D$
$4s4d\,{}^3D_2$	100,100,100,100,100,100% $4s4d\,{}^3D$
$4s4d\,{}^1D_2$	89,90,90,91,91,91% $4s4d\,{}^1D$; 11,10,10,9,9,9% $4p^2\,{}^1D$
$4s4d\,{}^3D_3$	100,100,100,100,100,100% $4s4d\,{}^3D$

TABLE X. Fitted and Hartree-Fock parameters (in cm^{-1}) for $4s5s$. Values arranged as in Table VIII. HF values were calculated with the Froese code, Ref. 28.

	Rb VIII	Sr IX	Y X	Zr XI	Nb XII	Mo XIII
$E_{av}(4s5s)$	525 387	614 837	709 632	809 809	915 331	1 026 304
	505 581	592 973	685 465	783 031	885 652	993 313
	1.039	1.037	1.035	1.035	1.034	1.033
$G^0(4s5s)$	5905	6338	6692	6955	7167	7281
	6390	6972	7543	8105	8660	9209
	0.925	0.909	0.887	0.858	0.828	0.791

TABLE XI. Fitted and Hartree-Fock parameters (in cm^{-1}) for $4s5d$. Values arranged as in Table VIII. HF values were calculated with the Froese code, Ref. 28.

	Y X	Zr XI	Nb XII	Mo XIII
$E_{av}(4s5d)$	914 318±60	1 037 113±80	1 165 594±130	1 300 047±69
	876 472	994 475	1 117 516	1 245 576
	1.043	1.043	1.043	1.044
$G^2(4s5d)$	10 182[a]	10 502[a]	10 792[a]	11 060[a]
	12 727	13 129	13 490	13 825
	0.80	0.80	0.80	0.80
ζ_{5d}	639±52	853±67	1089±108	1312±56
	419	536	673	831
	1.53	1.59	1.62	1.58
σ	95	125	203	107

[a]Fixed at 80% of HF value.

TABLE XII. Fitted and Hartree-Fock parameters (in cm^{-1}) for $4s4p$. Values arranged as in Table VIII. HF values were calculated with the Froese code, Ref. 28.

	Rb VIII	Sr IX	Y X	Zr XI	Nb XII	Mo XIII
$E_{av}(4s4p)$	151 685±12	168 358±14	185 289±17	202 546±21	220 128±25	238 113±29
	131 302	145 243	159 116	172 937	186 716	200 472
	1.155	1.159	1.164	1.171	1.179	1.188
$G^1(4s4p)$	76 547±41	82 501±50	88 358±61	94 102±73	99 827±89	105 502±105
	100 323	107 175	113 846	120 371	126 778	133 085
	0.763	0.770	0.776	0.782	0.787	0.793
ζ_{4p}	7 757±20	9 659±24	11 834±28	14 304±34	17 099±40	20 238±47
	6 733	8 438	10 389	12 605	15 108	17 918
	1.152	1.145	1.139	1.135	1.132	1.128
σ	22	26	32	38	45	53

TABLE XIII. Fitted and Hartree-Fock parameters (in cm^{-1}) for $4s5p+4p5s$. Values arranged as in Table VIII. HF values were calculated with the Froese code, Ref. 28.

	Sr IX	Y X	Zr XI	Nb XII	Mo XIII
$E_{av}(4s5p)$	687 727±152	791 183±15	900 309±15	1 015 040±24	1 135 426±19
	656 343	756 186	861 124	971 136	1 086 206
	1.048	1.046	1.046	1.045	1.045
$G^1(4s5p)$	9456±510	10 045±51	10 980±54	11 978±86	12 988±72
	10 803	11 438	12 062	12 677	13 287
	0.875	0.878	0.910	0.945	0.977
ζ_{5p}	3122[a]	3934[a]	4868[a]	5935[a]	7146[a]
$E_{av}(4p5s)$	800 202±97	912 891±9	1 031 390±9	1 155 598±14	1 285 665±12
	758 444	865 540	977 658	1 094 790	1 216 929
	1.055	1.055	1.055	1.056	1.056
$G^1(4p5s)$	4957±457	5823±44	6516±45	7181±71	7957±58
	10 405	11 143	11 872	12 594	13 309
	0.476	0.523	0.549	0.570	0.598
ζ_{4p}	9790±139	12 088±13	14 588±13	17 431±20	20 574±17
	8801	10 789	13 045	15 590	18 445
	1.11	1.12	1.12	1.12	1.12
$R^1(4s5p,4p5s)$	42 482[b]	46 061[b]	49 559[b]	52 989[b]	56 362[b]
	53 103	57 576	61 949	66 236	70 452
	0.80	0.80	0.80	0.80	0.80
$R^0(4s5p,5s4p)$	6144[b]	6598[b]	7049[b]	7496[b]	7941[b]
	7680	8248	8811	9370	9926
	0.80	0.80	0.80	0.80	0.80
σ	178	17	17	27	22

[a]Fixed at HF value.

[b]Fixed at 80% of HF value.

TABLE XIV. Ionization energies of Zn-like ions from Rb VIII to Mo XIII.

Ion	Series	Δn^* (calc)	Δn^* (adjusted)	Ionization energy (cm^{-1})	Ionization energy adopted (cm^{-1})	(eV)
Rb VIII	$4s^2,4s5s$	1.0174	1.0174(10)	1 070 100(500)	1 071 000(2000)	132.79(25)
Sr IX	$4s^2,4s5s$	1.0173	1.0169(10)	1 276 000(500)	1 277 000(2000)	158.33(25)
	$4s4p,4s5p$	1.0513	1.0499(10)	1 278 200(500)		
	$4p4s,4p5s$	1.0428	1.0424(10)	1 278 100(600)		
Y X	$4s^2,4s5s$	1.0170	1.0168(10)	1 496 800(700)	1 498 000(3000)	185.77(37)
	$4s4p,4s5p$	1.0487	1.0476(10)	1 498 800(600)		
	$4s4d,4s5d$	1.0339	1.0307(10)	1 496 600(500)		
	$4p4s,4p5s$	1.0406	1.0404(10)	1 499 000(700)		
Zr XI	$4s^2,4s5s$	1.0168	1.0169(10)	1 732 300(800)	1 733 000(3000)	214.86(37)
	$4s4p,4s5p$	1.0464	1.0458(10)	1 734 400(700)		
	$4s4d,4s5d$	1.0329	1.0307(10)	1 731 800(600)		
	$4p4s,4p5s$	1.0387	1.0388(10)	1 735 000(800)		
Nb XII	$4s^2,4s5s$	1.0164	1.0161(10)	1 983 400(900)	1 985 000(3000)	246.11(37)
	$4s4p,4s5p$	1.0443	1.0434(10)	1 985 500(800)		
	$4s4d,4s5d$	1.0318	1.0294(10)	1 982 800(700)		
	$4p4s,4p5s$	1.0370	1.0367(10)	1 986 400(900)		
Mo XIII	$4s^2,4s5s$	1.0161	1.0151(10)	2 249 900(1100)	2 251 000(4000)	279.09(50)
	$4s4p,4s5p$	1.0424	1.0409(10)	2 252 000(900)		
	$4s4d,4s5d$	1.0308	1.0278(10)	2 249 400(800)		
	$4p4s,4p5s$	1.0352	1.0342(10)	2 253 600(1000)		

the different series. The adopted value for Rb VIII was taken to be 1000 cm^{-1} higher than the value found from the $4s^2$, $4s5s$ series because of the trend for this value to be about this amount lower than the average in the other ions. Our experimental ionization energies are about 2 eV higher than the pure HF ionization energies of Fraga *et al.*[34] and about 10 eV lower than the relativistic HF values of Carlson *et al.*[35]

The fundamental parts of the term systems of ions in the Zn isoelectronic sequence are now well known for most ions up to Mo XIII. The most important parts that are still missing are the configurations $4s4f$ and $4p4d$. We have made some tentative identifications, and the analysis of the spectrograms will continue. Work to extend the sequence to higher charge states is also in progress.

Note added in proof. After this paper was submitted for publication a paper appeared by J.-F. Wyart and M.-C. Artru, Phys. Lett. A **21**, 419 (1987), reporting wavelengths and energy levels for the $4s^2$, $4s4p$, $4p^2$, and $4s4d$ configurations of Sr IX. Our line classifications agree. Our wavelengths for the $n=4-4$ transitions are about 0.010 Å lower than theirs. Our values for the levels of the $n=4$ configurations are higher than theirs by amounts varying up to about 10 cm^{-1}. A paper has also appeared by J.-F. Wyart, P. Mandelbaum, M. Klapisch, J. L. Schwob, and N. Schweitzer, Phys. Scr. **36**, 224 (1987), reporting $n=4-5$ transitions for zinclike ions from Y X to Sn XXI. Where our results overlap they are in fairly good agreement. In their spectrum of Mo XIII the $4s4p\ ^3P_0-4s5s\ ^3S_1$ transition is blended with a strong line of Mo XIV at 121.644 Å. In our spectrum this transition is observed as a separate line at 121.597 Å.

ACKNOWLEDGMENTS

U.L. is grateful to the staff of the National Bureau of Standards, Atomic Spectroscopy Group, for hospitality during his stay as a guest worker in 1987. This work was supported by the Swedish Natural Science Research Council, the Swedish Energy Research Commission, the Office of Magnetic Fusion Energy of the U.S. Department of Energy, and the Innovative Science and Technology/Strategic Defense Initiative Organization under direction of the Naval Research Laboratory.

[1]U. Litzén and K. Ando, Phys. Lett. **100A**, 411 (1984).
[2]E. Alexander, M. Even-Zohar, B. S. Fraenkel, and S. Goldsmith, J. Opt. Soc. Am. **61**, 508 (1971).
[3]E. Hinnov, L. C. Johnson, E. B. Meservey, and D. L. Dimock, Plasma Phys. **14**, 755 (1972).
[4]E. Hinnov, Phys. Rev. A **14**, 1533 (1976).
[5]J. Reader and N. Acquista, Phys. Rev. Lett. **39**, 184 (1977).
[6]M. Finkenthal, R. E. Bell, H. W. Moos, A. K. Bhatia, E. S. Marmar, J. L. Terry, and J. E. Rice, Phys. Lett. **82A**, 123 (1981).
[7]P. G. Burkhalter, J. Reader, and R. D. Cowan, J. Opt. Soc. Am. **70**, 912 (1980).
[8]J.-F. Wyart, J. Reader, and A. N. Ryabtsev, J. Opt. Soc. Am. **71**, 692 (1981).
[9]N. Acquista and J. Reader, J. Opt. Soc. Am. **71**, 569 (1981).
[10]J.-F. Wyart, Th. A. M. van Kleef, A. N. Ryabtsev, and Y. N. Joshi, Phys. Scr. **29**, 319 (1984).
[11]S. Goldsmith, J. Reader, and N. Acquista, J. Opt. Soc. Am. B **1**, 631 (1984).
[12]J. Reader and N. Acquista, J. Opt. Soc. Am. **69**, 1285 (1979).
[13]J. Reader and N. Acquista, J. Opt. Soc. Am. **69**, 1659 (1979).
[14]J. Reader and N. Acquista, J. Opt. Soc. Am. **70**, 317 (1980).
[15]J. Reader, G. Luther, and N. Acquista, J. Opt. Soc. Am. **69**, 144 (1979).
[16]J. Reader, G. Luther, and N. Acquista, J. Opt. Soc. Am. **71**, 204 (1981).
[17]V. Kaufman and B. Edlén, J. Phys. Chem. Ref. Data **3**, 825 (1974).
[18]R. L. Kelly and L. J. Palumbo, *Atomic and Ionic Emission Lines Below 2000 Angstroms—Hydrogen Through Krypton* (U.S. GPO, Washington, D.C., 1973).
[19]S.-G. Pettersson, Phys. Scr. **26**, 296 (1982).
[20]B. Isberg, Ark. Fys. **35**, 551 (1967).
[21]J. Reader, J. Opt. Soc. Am. **65**, 286 (1975).
[22]J. Reader and G. L. Epstein, J. Opt. Soc. Am. **62**, 1467 (1972).
[23]W. Persson and C.-G. Wahlstrom, Phys. Scr. **31**, 487 (1985).
[24]W. Persson and S.-G. Pettersson, Phys. Scr. **29**, 308 (1984).
[25]The computer program ELCALC was written by L. J. Radziemski, Jr., Los Alamos National Laboratory, Los Alamos, New Mexico 87544.
[26]R. D. Cowan, *The Theory of Atomic Structure and Spectra* (University of California Press, Berkeley, 1981).
[27]E. P. Ivanova, L. N. Ivanov, A. D. Gurchumelya, M. A. Tsirekidze, and T. A. Tsirekidze, J. Phys. B **18**, 1467 (1985).
[28]C. Froese Fischer, Comput. Phys. Commun. **4**, 107 (1972).
[29]C. Froese Fischer and J. E. Hansen, Phys. Rev. A **19**, 1819 (1979).
[30]B. Isberg and U. Litzén, Phys. Scr. **31**, 533 (1985).
[31]C. E. Moore, *Atomic Energy Levels,* Natl. Bur. Stand. (U.S.) Circ. No. 467 (U.S. GPO, Washington D.C., 1952), Vol. II.
[32]Y. N. Joshi and Th. A. M. van Kleef, Phys. Scr. **34**, 135 (1986).
[33]L. J. Curtis, Phys. Rev. A **35**, 2089 (1987).
[34]S. Fraga, J. Karwowski, and K. M. S. Saxena, *Handbook of Atomic Data* (Elsevier, New York, 1976).
[35]T. A. Carlson, C. W. Nestor Jr., N. Wasserman, and J. D. McDowell, At. Data Nucl. Data Tables **2**, 63 (1970).